Analog Grover search by adiabatic passage in a cavity-laser-atom system

D. Daems*
QuIC, Ecole Polytechnique, Université Libre de Bruxelles, 1050 Bruxelles, Belgium

S. Guérin†
Institut Carnot de Bourgogne UMR 5209 CNRS, Université de Bourgogne, BP 47870, 21078 Dijon, France
(Received 10 June 2008; published 20 August 2008)

A physical implementation of the adiabatic Grover search is theoretically investigated in a system of N identical three-level atoms trapped in a single-mode cavity. Some of the atoms are marked through the presence of an energy gap between their two ground states. The search is controlled by two partially delayed lasers which allow a deterministic adiabatic transfer from an initially entangled state to the marked states. Pulse schemes are proposed to satisfy the Grover speedup either exactly or approximately, and the success rate of the search is calculated.

DOI: 10.1103/PhysRevA.78.022330 PACS number(s): 03.67.Lx, 32.80.Qk, 42.50.−p

I. INTRODUCTION

Search problems can be expressed as finding a set of marked items in an unsorted list. The Grover algorithm [1] achieves this task quadratically faster than a classical algorithm, which examines items one by one. It has become a paradigm of quantum computation based on quantum circuits. The case of two qubits, corresponding to a four-element search, has been demonstrated experimentally in various settings. NMR experiments [2–4] used the spin states of ^{1}H and/or ^{13}C in a magnetic field as qubits while radio-frequency fields and spin-spin couplings between the nuclei were used to implement quantum logic gates. In linear optics techniques, the individual qubits are represented by different polarization or spatial-mode degrees of freedom, while the computation is achieved through essentially a complicated interferometer [5] or a one-way quantum computer [6]. Trapped-ion systems [7], which present the advantage of being scalable, rely on a number of optical and microwaves sources to control, entangle, and measure the qubits which are represented by the ground-state hyperfine levels of two trapped atomic ions. There have also been proposals of experimental implementations using cavity QED where the quantum gate dynamics is provided by a cavity-assisted collision [8] or by a strong resonant classical field [9].

A different approach to quantum computation consists in the controlled evolution of a system obeying the Schrödinger equation with a Hamiltonian designed to solve a specified problem. It was pioneered by Farhi and Gutmann [10] who considered a time-continuous version of the Grover algorithm. A given Hamiltonian features a marked state whose energy differs from that of the $N-1$ unmarked ones. A driving Hamiltonian is then constructed, without any knowledge of the solution, to produce a Rabi-like half-cycle which populates the marked state in a time scaling as $N^{1/2}$, thereby exhibiting the quadratic speedup. An experimental realization of this analog Grover algorithm has been performed by NMR [11] in a setting where a quadrupolar coupling makes a spin-3/2 nucleus a two-qubit system ($N=4$).

Adiabatic processes offer many advantages—in particular, the high degree of population transfer and some robustness with respect to fluctuations of the control fields or imperfect knowledge of the model. Adiabatic versions of the time-continuous Grover algorithm have been constructed in abstract form [12–14]. An *ad hoc* Hamiltonian connects adiabatically the initial ground superposition to the marked state through an effective two-state avoided crossing. It has been shown [14] that the transfer to the marked state in a time growing as $N^{1/2}$ requires a specific time-dependent sweeping of the parameter controlling the Hamiltonian. We have recently proposed a physical implementation of such an adiabatic search using three-state atoms trapped in a QED cavity and driven by laser fields [15]. This scheme leads to an effective three-state dynamics which is closely related to stimulated Raman adiabatic passage (STIRAP) [16]. We have determined analytically the shapes of the adiabatic pulses that are required to lead to a quadratic speedup of the search.

The present work contains a detailed description of the techniques and results announced in Ref. [15]. We consider the more general case of search problems which have more than one solution. The dynamics of the collective marked, unmarked, and excited states introduced below is solved exactly under local adiabatic conditions for which the scaling is determined analytically. Furthermore, we study numerically the robustness of the Grover search in this system using pulses which are easily generated in practice (typically Gaussian pulses with plateaus). We identify the pertaining conditions which give rise to a speedup of the search which is only approximately quadratic in this case.

The paper is organized as follows. In Sec. II, we describe the cavity-laser-atom system, introduce the relevant collective states, and derive the effective Hamiltonian. Section III is devoted to the analysis of the adiabatic conditions leading to a Grover search with an exact or approximate quadratic speedup. The two types of pulses schemes are illustrated and discussed in Sec. IV, while the conclusions are given in Sec. V.

*ddaems@ulb.ac.be
†sguerin@u-bourgogne.fr

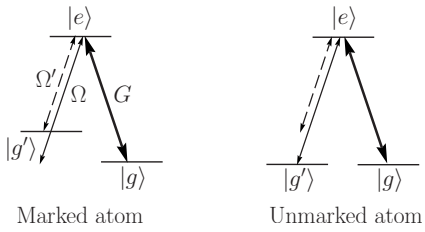

FIG. 1. Linkage pattern for the individual atoms. The unmarked atoms have two degenerate ground states $|g\rangle$ and $|g'\rangle$. The marked atoms feature the state $|g'\rangle$ shifted. The laser of Rabi frequency Ω' (Ω) is resonant with the g'-e transition for the marked (unmarked) atoms. The cavity of Rabi frequency G is resonant with the g-e transition.

II. CAVITY-LASER-ATOM SYSTEM

A. Description

We use an ensemble of N identical three-level atoms trapped in a single-mode cavity of coupling frequency G and driven by two lasers of Rabi frequencies Ω and Ω'. The key of the search process is that all the atoms have to be entangled initially as defined below. The atoms have a Λ configuration with two ground Zeeman states $|g\rangle$ and $|g'\rangle$, coupled to the excited state $|e\rangle$ by, respectively, the cavity and the two lasers (see Fig. 1). The states $|g'\rangle$ of all the atoms are considered as the database. The state $|g\rangle$ stands here to couple all the atoms together by exchanging a single photon in the cavity. It allows us to consider the unmarked collective state, defined as the normalized sum of all the possible states $|g'_j\rangle$ for all the unmarked atoms in state $|g\rangle$ except the jth in $|g'\rangle$. The state $|g'\rangle$ of any marked atom is shifted—for instance, by a magnetic field—such that the transition g'-e is resonant with the laser Ω' (Ω) for a marked atom (unmarked atom). In this scheme, the magnetic field should be atomic selective and the atoms should thus be fixed and form a register (of one or two dimension) in the cavity. We start from the initial entangled state $|g',0\rangle \equiv (1/\sqrt{N})\Sigma_{j=1}^{N}|g'_j,0\rangle$ featuring a collective superposition of both types of ground states. Such a state can be prepared, for instance, before the marking of the atom using the STIRAP technique, exactly as shown by Fleischhauer and Lukin to store single-photon quantum states [17]. In their scheme, a single-photon wave packet enters the cavity through a mirror while the resonant laser Ω is on and strong as $\Omega \gg G\sqrt{N}$, and the atoms are all in their ground state $g\rangle$. This generates the state denoted $|g,1\rangle$. The laser is next switched off adiabatically while the photon is in the cavity, such that the population is transferred by STIRAP from the state $|g,1\rangle$ to the collective state $|g',0\rangle$. In this final state the photon is stored, shared among all the atoms.

A related adiabatic process is constructed here in order to transfer adiabatically the initial entangled state $|g',0\rangle$ to a superposition of the marked states using an inverse fractional STIRAP (if-STIRAP). This if-STIRAP is the time inversion of the fractional STIRAP (f-STIRAP) which transfers population from a single state to a superposition of states [18]. The if-STIRAP allows one here to transfer the population from the superposition $|g',0\rangle$ to the marked state.

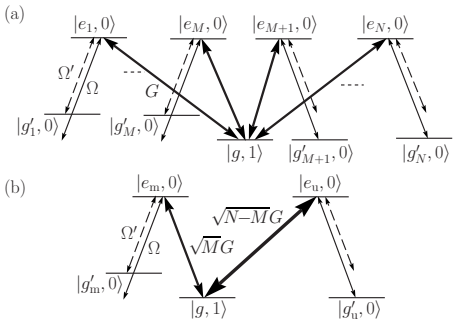

FIG. 2. (a) Coupling scheme in the cavity. The cavity G, laser Ω, and laser Ω' Rabi frequency are featured by, respectively, thick, thin, and dashed arrows. (b) Equivalent scheme where the states $|g'_i,0\rangle$ and $|e_i,0\rangle$), $i=1,M$ $[i=M+1,N]$ of frame (a) form the collective marked ground ($|g'_m,0\rangle$) and excited ($|e_m,0\rangle$) states [the collective unmarked ground ($|g'_u,0\rangle$) and excited ($|e_u,0\rangle$) states]. The effective cavity Rabi frequency to the collective marked (unmarked) excited state is $\sqrt{M}G$ ($\sqrt{N-M}G$).

B. Model Hamiltonian

The Hamiltonian describing the system of N atoms is

$$H_0 = \delta\sum_{j=1}^{M}|g'_j\rangle\langle g'_j| + \omega\sum_{j=1}^{N}|e_j\rangle\langle e_j|. \tag{1}$$

We consider a cavity mode of frequency ω and coupling strength G together with two lasers of frequencies ω and $\omega - \delta$ and pulse shapes $\Omega(t)$ and $\Omega'(t)$ which do not grow with N. The resonant driving provided by the cavity-laser-atom system is described by

$$V = \omega a^{\dagger}a + Ga\sum_{j=1}^{N}|e_j\rangle\langle g_j| + [\Omega e^{i\omega t} + \Omega' e^{i(\omega-\delta)t}]\sum_{j=1}^{N}|g'_j\rangle\langle e_j| + \text{H.c.} \tag{2}$$

The full Hamiltonian $H=H_0+V$ is block diagonal. Each block may be labeled by the number k of photons which are present in the cavity when the N atoms are in their ground state $|g\rangle$. The corresponding multipartite state $|g_1\cdots g_N\rangle \otimes |k\rangle$ is denoted $|g,k\rangle$. All the states which are coupled to $|g,k\rangle$ span a subspace whose projection operator is $\mathcal{P}_k$. The Hamiltonian may thus be rewritten as $H=\Sigma_{k=0}\mathcal{P}_k H\mathcal{P}_k$. We shall focus on the block $\mathcal{P}_1 H\mathcal{P}_1$ associated with a single photon in the cavity.

The multipartite state $|g,1\rangle$ is coupled by the cavity to any state $|g_1\cdots g_{j-1}e_j g_{j+1}\cdots\rangle \otimes |0\rangle \equiv |e_j,0\rangle$ for which the atom j is in its excited state while the other atoms remain in their ground state $|g\rangle$. Each state $|e_j,0\rangle$ is coupled by the laser to the state $|g_1\cdots g_{j-1}g'_j g_{j+1}\cdots g_N\rangle \otimes |0\rangle \equiv |g'_j,0\rangle$ where the atom j is in the ground state $|g'\rangle$ while the other atoms are in the ground state $|g\rangle$. This coupling scheme is illustrated in Fig. 2(a), and the corresponding projection operator, spanning this subspace closer under H, reads

$$\mathcal{P}_1 = \sum_{j=1}^{N}(\mathcal{P}_{|g'_j,0\rangle} + \mathcal{P}_{|e_j,0\rangle}) + \mathcal{P}_{|g,1\rangle}. \tag{3}$$

C. Collective marked and unmarked dressed states

In order to remove the oscillatory time dependence introduced by diagonal terms, we consider atomic states which are dressed by laser and cavity photons through the resonant transformation

$$R = e^{-i\delta t}\sum_{j=1}^{M} |g'_j,0\rangle\langle g'_j,0| + \sum_{j=M+1}^{N} |g'_j,0\rangle\langle g'_j,0| + e^{-i\omega t}|g,1\rangle\langle g,1| + e^{-i\omega t}\sum_{j=1}^{N} |e_j,0\rangle\langle e_j,0|. \quad (4)$$

This results in the new Hamiltonian

$$H_R = R^\dagger(\mathcal{P}_1 H \mathcal{P}_1)R - iR^\dagger \dot{R}, \quad (5)$$

where the overdot denotes time derivative.

Among the marked atoms, none plays a privileged role. Similarly, the unmarked atoms are all equivalent. It is therefore appealing to treat them collectively. We consider the uniform superposition of marked (unmarked) ground states

$$|g'_{\mathrm{m}},0\rangle = \frac{1}{\sqrt{M}}\sum_{j=1}^{M} |g'_j,0\rangle,$$

$$|g'_{\mathrm{u}},0\rangle = \frac{1}{\sqrt{N-M}}\sum_{j=M+1}^{N} |g'_j,0\rangle, \quad (6)$$

and the uniform superposition of excited states associated with the marked (unmarked) atoms

$$|e_{\mathrm{m}},0\rangle = \frac{1}{\sqrt{M}}\sum_{j=1}^{M} |e_j,0\rangle.$$

$$|e_{\mathrm{u}},0\rangle = \frac{1}{\sqrt{N-M}}\sum_{j=M+1}^{N} |e_j,0\rangle. \quad (7)$$

These states, together with $|g,1\rangle$, define a subspace which is relevant for the Grover search. Indeed, it can be shown that this subspace is closed under H_R,

$$H_R = \mathcal{P}H_R\mathcal{P} + (I-\mathcal{P})H_R(\mathcal{P}_1 - \mathcal{P}), \quad (8)$$

where

$$\mathcal{P} = \mathcal{P}_{|g'_{\mathrm{m}},0\rangle} + \mathcal{P}_{|g'_{\mathrm{u}},0\rangle} + \mathcal{P}_{|e_{\mathrm{m}},0\rangle} + \mathcal{P}_{|e_{\mathrm{u}},0\rangle} + \mathcal{P}_{|g,1\rangle}. \quad (9)$$

We may thus restrict our attention to the Hamiltonian

$$H_1 \equiv \mathcal{P}H_R\mathcal{P} = G(\sqrt{M}|e_{\mathrm{m}},0\rangle + \sqrt{N-M}|e_{\mathrm{u}},0\rangle)\langle g,1| + \Sigma'|g'_{\mathrm{m}},0\rangle\langle e_{\mathrm{m}},0| + \Sigma|g'_{\mathrm{u}},0\rangle\langle e_{\mathrm{u}},0| + \mathrm{H.c.}, \quad (10)$$

where $\Sigma = \Omega + e^{-i\delta t}\Omega'$ and $\Sigma' = \Omega' + e^{i\delta t}\Omega$. This Hamiltonian is schematically represented in Fig. 2(b).

D. Effective Hamiltonian

The Hamiltonian H_1 can be rewritten in a way which is prone to a further reduction. Indeed, notice that the first term of (10) actually features a linear combination of $|e_{\mathrm{m}},0\rangle$ and $|e_{\mathrm{u}},0\rangle$ which is nothing but the uniform superposition over all atoms, $\frac{1}{\sqrt{N}}\Sigma_{j=1}^{N}|e_j,0\rangle \equiv |e,0\rangle$. This is expected since the state $|g,1\rangle$ is coupled indifferently to any of the state $|e_j,0\rangle$, marked or not, as is seen for instance in Fig. 2(a). By contrast, owing to the detuning, the g'-e transitions are not equivalent in the marked and unmarked cases. Hence, the last two terms of (10) involve either $|e_{\mathrm{m}},0\rangle$ or $|e_{\mathrm{u}},0\rangle$. We may express H_1 in terms of $|e,0\rangle$ and a state $|e_\perp,0\rangle$ which is orthogonal to the uniform superposition,

$$|e,0\rangle = \sqrt{f}|e_{\mathrm{m}},0\rangle + \sqrt{1-f}|e_{\mathrm{u}},0\rangle,$$

$$|e_\perp,0\rangle = \sqrt{1-f}|e_{\mathrm{m}},0\rangle - \sqrt{f}|e_{\mathrm{u}},0\rangle, \quad f \equiv \frac{M}{N}. \quad (11)$$

The result reads

$$H_1 = H_{e_\perp} + H_e + H_{e_\perp e} + H_{ee_\perp}, \quad (12)$$

where H_e and $H_{e_\perp}$ are coupled to each other only through $H_{e_\perp e}$ and $H_{ee_\perp} = H^\dagger_{e_\perp e}$,

$$H_{e_\perp} = \sqrt{1-f}\Sigma'|g'_{\mathrm{m}},0\rangle\langle e_\perp,0| - \sqrt{f}\Sigma|g'_{\mathrm{u}},0\rangle\langle e_\perp,0| + \mathrm{H.c.},$$

$$H_e = \sqrt{N}G|e,0\rangle\langle g,1| + \mathrm{H.c.},$$

$$H_{e_\perp e} = \sqrt{f}\Sigma'|g'_{\mathrm{m}},0\rangle\langle e,0| + \sqrt{1-f}\Sigma|g'_{\mathrm{u}},0\rangle\langle e,0|. \quad (13)$$

As just mentioned, it is the Hamiltonian $H_{e_\perp}$ which discriminates the marked and unmarked states whereas H_e only features uniform superpositions over all the atoms. The subspace of interest is thus spanned by the projector

$$\mathcal{P}_{e_\perp} = \mathcal{P}_{|g'_{\mathrm{m}},0\rangle} + \mathcal{P}_{|g'_{\mathrm{u}},0\rangle} + \mathcal{P}_{|e_\perp\rangle}. \quad (14)$$

With the help of a unitary transformation $T = \exp(W)$ we can perturbatively block-diagonalize the Hamiltonian H_1. In this relevant subspace, the first correction to $H_{e_\perp}$ is obtained by the partitioning technique, which is recalled in the Appendix, as $\frac{1}{2}\mathcal{P}_{e_\perp}[H_{ee_\perp}, \varepsilon W]\mathcal{P}_{e_\perp}$. This quantity, featuring denominators which are the difference of the eigenvalues of $H_{e_\perp}$ and H_e, decreases at least as $1/NG^2$ (with additional decreasing contributions due to f). As a consequence, we shall neglect this correction together with the nonresonant components in Σ and Σ'. We therefore consider the effective Hamiltonian

$$H_{\mathrm{eff}} = \sqrt{1-f}\Omega'|g'_{\mathrm{m}},0\rangle\langle e_\perp,0| - \sqrt{f}\Omega|g'_{\mathrm{u}},0\rangle\langle e_\perp,0| + \mathrm{H.c.}, \quad (15)$$

which is schematically depicted in Fig. 3.

III. GROVER SEARCH

A. Starting and final points

Our aim is to transfer adiabatically the population from the initial state $|g',0\rangle$,

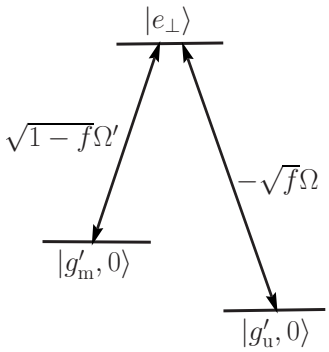

FIG. 3. Coupling scheme in the Λ system corresponding to the effective Hamiltonian (15) with a fraction f $(=M/N)$ of solution to the search problem.

$$|g',0\rangle \equiv \frac{1}{\sqrt{N}}\sum_{j=1}^{N}|g'_j,0\rangle, \tag{16}$$

which gives no privileged role to any of the N states $|g'_j,0\rangle$ to a final state which coincides with the collective marked state $|g'_{\rm m},0\rangle$ in a time which scales as $\sqrt{1/f}$ where $f=M/N$ is the fraction of solutions. The population transfer mechanism is most easily revealed in the basis of the instantaneous eigenstates of $H_{\rm eff}(t)$,

$$|0\rangle(t) = \cos\,\theta(t)|g'_{\rm m},0\rangle - \sin\,\theta(t)|g'_{\rm u},0\rangle$$

$$|\pm\Lambda\rangle(t) = \frac{1}{\sqrt{2}}[\sin\,\theta(t)|g'_{\rm m},0\rangle + \cos\,\theta(t)|g'_{\rm u},0\rangle \pm |e_\perp,0\rangle], \tag{17}$$

pertaining to the eigenvalues 0 and $\pm\Lambda(t)$ where

$$\Lambda(t) = \sqrt{(1-f)\Omega'^2(t) + f\Omega^2(t)}. \tag{18}$$

Note that $|0\rangle$ has no component on the collective excited states $|e_\perp,0\rangle$ and is therefore a so-called dark state, which is immune to loss by spontaneous emission (in contrast to the states $|\pm\Lambda\rangle$). The instantaneous angle $\theta(t)$ is defined through the relation

$$\tan\,\theta(t) = -\sqrt{\frac{1-f}{f}}\frac{\Omega'(t)}{\Omega(t)}. \tag{19}$$

Requiring the instantaneous eigenstate (17) to coincide at the initial time $t_{\rm i}$ with the uniform superposition

$$|g',0\rangle = \sqrt{f}|g'_{\rm m},0\rangle + \sqrt{1-f}|g'_{\rm u},0\rangle \tag{20}$$

and at the final time with the collective marked state $|g'_{\rm m},0\rangle$ entails that

$$\tan\,\theta(t_{\rm i}) = -\sqrt{\frac{1-f}{f}}, \quad \tan\,\theta(t_{\rm f}) = 0. \tag{21}$$

This implies that the two pulses must be switched on simultaneously, $\Omega'(t_{\rm i})=\Omega(t_{\rm i})$, and that the pulse Ω' is to be turned off before Ω. This process can be named if-STIRAP since it allows the transfer by a STIRAP-type process from a superposition of states to a single state [16]. In the adiabatic representation (17), the effective Hamiltonian reads

$$H_{\rm eff}^{\rm ad} = \Lambda(|+\Lambda\rangle\langle+\Lambda| + |-\Lambda\rangle\langle-\Lambda|) + \frac{i\dot{\theta}}{\sqrt{2}}(|+\Lambda\rangle\langle 0| + |-\Lambda\rangle\langle 0| - \text{H.c.}), \tag{22}$$

where $\dot{\theta}=\frac{1}{1+\tan^2\theta}\frac{d}{dt}\tan\,\theta$. In the adiabatic regime, the transitions between instantaneous eigenstates are negligible. This will be achieved if the Hamiltonian varies sufficiently slowly in time so as to keep $\dot{\theta}\ll\Lambda$. On the other hand, we wish to control the process duration and, in particular, to prevent it from becoming arbitrarily large. This can be achieved in several ways, two of which shall be considered explicitly.

B. Local adiabatic conditions

In order to control the process duration, as proposed in [14], we choose to require $\dot{\theta}$ and Λ to be in a constant (small) ratio ε at all times, independently of N:

$$\dot{\theta} = \varepsilon\Lambda. \tag{23}$$

Given a laser pulse Ω, this equation will allow us to determine the pulse Ω' which is needed to remain in the instantaneous eigenstate $|0\rangle(t)$ with a significant probability throughout the process, starting from the uniform superposition $|0\rangle(t_{\rm i})=|g',0\rangle$ and ending up in the marked state $|0\rangle(t_{\rm f})=|g'_{\rm m},0\rangle$ after some time $t_{\rm f}$-$t_{\rm i}$ which achieves the optimal scaling with N.

Indeed, let us first rewrite Λ defined in (18) in terms of $\tan\,\theta$ through (19) as

$$\Lambda = \sqrt{f}\sqrt{1+\tan^2\theta}\Omega. \tag{24}$$

We then obtain from (23) a differential equation for $\tan\,\theta$—i.e., for the ratio Ω'/Ω:

$$\frac{d\,\tan\,\theta}{(1+\tan^2\,\theta)^{3/2}} = \varepsilon\sqrt{f}\Omega\,dt. \tag{25}$$

Its solution satisfying the initial condition (21) reads

$$\frac{\Omega'(t)}{\Omega(t)} = \frac{1-\varepsilon\mathcal{A}(t)\sqrt{\dfrac{f}{1-f}}}{\sqrt{1+\varepsilon\mathcal{A}(t)\left\{2\sqrt{\dfrac{1-f}{f}}-\varepsilon\mathcal{A}(t)\right\}}}, \tag{26}$$

where we define $\mathcal{A}(t)\equiv\int_{t_{\rm i}}^{t}du\,\Omega(u)$. Upon specifying that at time $t_{\rm f}$ the ratio of the pulses vanishes, one deduces from (26) that $\varepsilon\mathcal{A}(t_{\rm f})=\sqrt{(1-f)/f}$. Expressing the total area of the pulse Ω in terms of its peak amplitude Ω_0 and the process duration $\mathcal{T}$, $\mathcal{A}(t_{\rm f})=\Omega_0\mathcal{T}$, we finally obtain

$$\Omega_0\mathcal{T} = \frac{1}{\varepsilon}\sqrt{\frac{1-f}{f}}. \tag{27}$$

This expression shows that the search duration scales as $f^{-1/2}$ for a peak amplitude which is independent of $f=M/N$.

Equivalently, we can increase the peak amplitude as $f^{-1/2}$ for a constant duration $\mathcal{T}$.

We now determine the population which can be reached by adiabatic passage. With the choice (23), we see from (22) that Λ appears as factor in the Hamiltonian $H_{\rm eff}^{\rm ad}$. Hence, we can define a new time $\tau(t)=\int_{t_i}^{t} ds\,\Lambda(s)$ so that the Hamiltonian $H_{\rm eff}^{\rm ad}/\Lambda$ is time independent. It follows that the survival probability amplitude of the state $|0(t)\rangle$ is

$$\langle 0(t)|\exp\left(-i\tau(t)\frac{H_{\rm eff}^{\rm ad}}{\Lambda}\right)|0(t_i)\rangle=\frac{1+\varepsilon^2\cos\lambda\tau(t)}{1+\varepsilon^2}, \quad (28)$$

where $\lambda\equiv\sqrt{1+\varepsilon^2}$. The system therefore stays in the state $|0(t)\rangle$ with a probability satisfying at all times

$$P_0(t)\geqslant\left(\frac{1-\varepsilon^2}{1+\varepsilon^2}\right)^2\sim 1-4\varepsilon^2. \quad (29)$$

The nonadiabatic losses (to the states $|\pm\Lambda\rangle$ which contain some component on the excited state $|e_\perp\rangle$) are therefore never larger than $4\varepsilon^2$. Furthermore, since the states $|0\rangle$ and $|g_{\rm m}',0\rangle$ coincide at the final time, relation (29) also implies that the collective marked state ends up with a population of the order of $1-4\varepsilon^2$.

Returning to the diabatic representation, in which the state vector is denoted $|\phi(t)\rangle$, one can determine the full population dynamics of the collective states featured in the effective Hamiltonian (15). The population of the collective marked state is found to be

$$P_{\rm m}(t)\equiv|\langle g_{\rm m}',0|\phi(t)\rangle|^2=\left|\frac{\varepsilon}{\lambda}\sin\lambda\tau(t)\sin\theta(t)+\frac{1+\varepsilon^2\cos\lambda\tau(t)}{1+\varepsilon^2}\cos\theta(t)\right|^2, \quad (30)$$

where $\theta(t)$ is given by (19) and (26). Recalling from (21) that, at the final time, $\sin\theta(t_{\rm f})=0$, one deduces that

$$P_{\rm m}(t_{\rm f})=\left(\frac{1+\varepsilon^2\cos\lambda\tau(t_{\rm f})}{1+\varepsilon^2}\right)^2\geqslant\left(\frac{1-\varepsilon^2}{1+\varepsilon^2}\right)^2. \quad (31)$$

The population $P_{\rm u}(t)\equiv|\langle g_{\rm u}',0|\phi(t)\rangle|^2$ of the collective unmarked state is given by an expression similar to (30) where $\sin\theta(t)$ and $\cos\theta(t)$ are interchanged. In particular, this entails that, at the final time, it is of order ε^2,

$$P_{\rm u}(t_{\rm f})=\frac{\varepsilon^2}{1+\varepsilon^2}\sin^2\lambda\tau(t_{\rm f}). \quad (32)$$

Finally, the population of the collective excited state $|e_\perp\rangle$ is

$$P_{e_\perp}(t)=\frac{2\varepsilon^2}{(1+\varepsilon^2)^2}[1-\cos\lambda\tau(t)]^2, \quad (33)$$

which puts a bound on the decoherence present in the system since the population of this excited state is never larger than ε^2.

C. Tailored Gaussian pulses

The local adiabatic conditions considered in the preceding section allowed us to determine explicitly the scaling of the search duration and the population of the collective marked state. This is only a particular choice. The proposed scheme is robust in this respect. Indeed, as long as the initial and final conditions (21) are satisfied and one goes adiabatically from one to the other, the desired transfer of population can be achieved in a time which scales appropriately. In practical applications, it may be easier to consider Gaussian pulses possibly with plateaus.

In order to satisfy the initial condition, the two pulses Ω and Ω' that are used in the current scheme are to be turned on simultaneously. The pulse Ω' is a standard Gaussian pulse $\Omega'=\Omega_0 e^{-(t/T)^2}$. As for Ω, it has a Gaussian switching on, and when the peak is reached, the pulse is kept at this value for a time αT before being switched off according to a Gaussian,

$$\Omega=\begin{cases}\Omega_0 e^{-(t/T)^2}, & t\geqslant 0,\\ \Omega_0, & 0\leqslant t\leqslant\alpha T,\\ \Omega_0 e^{-(t/T-\alpha)^2}, & t\geqslant\alpha T.\end{cases} \quad (34)$$

We show numerically in the next section that with such pulses the search duration has a scaling which is close to optimal for $\alpha\gtrsim 1.5$.

IV. DISCUSSION

The current adiabatic search scheme is robust in the sense that it leaves some flexibility on the pulses that are used. We presented explicitly two choices of pulses which will now be illustrated and compared.

We first consider the case of (23) which amounts to requiring local adiabatic conditions. The pulses are determined by (26) and displayed in the upper panel of Fig. 4 for $f=M/N=3/8$, $\varepsilon=0.05$, and a Gaussian pulse Ω of characteristic duration T. This value of ε implies that the lower bound (29) of the probability P_0 of the system to remain in the instantaneous eigenstate is 0.99. The population dynamics of the collective marked, unmarked, and excited states is given by the analytical expressions (30)–(33) and is depicted in the lower panel. As predicted by (31), the transfer to the marked state is very efficient with a low transient population in the excited states stemming from the fact that the dynamics remains in the instantaneous decoherence-free eigenstate $|0\rangle(t)$ in the adiabatic limit. We remark that the choice (23), which leads to the seemingly complicated pulse relation (26), gives in practice a simple smooth bell-shaped pulse (see upper panel of Fig. 4). Increasing f (i.e., increasing M for a given N) allows the reduction of the pulse area with the same efficiency, as shown by (27).

We now turn to the case of tailored Gaussian pulses. Figures 5 and 6 show the dynamics for such pulses with $f=M/N=1/8$ and $f=3/8$, respectively. We have here chosen a plateau of duration $1.5T$ ($\alpha=1.5$). The pulse area of Ω' has been chosen such that the population transfer to the marked state is approximately 0.99 (i.e., as in the conditions of Fig. 4). Figures 5 and 6 show similar features as Fig. 4: low transient population in the excited states, comparable pulse area for the same efficiency, and reduction of the pulse area with the same efficiency for increasing M. We remark, however, on two different properties: (i) For a similar efficiency,

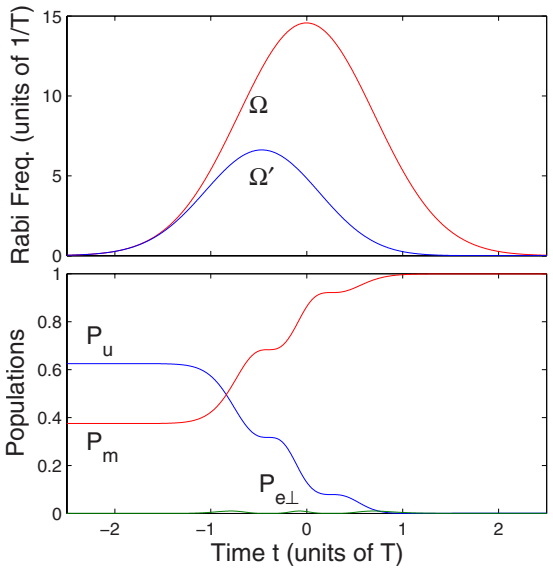

FIG. 4. (Color online) Analytical dynamics for the effective Hamiltonian (15) with $f=M/N=3/8$, $\varepsilon=0.05$, and Rabi frequencies given by a Gaussian profile $\Omega(t)=\Omega_0 e^{-(t/T)^2}$ and expression (26) for $\Omega'(t)$. Here $\Omega_0 T=\sqrt{(1-f)/f}/\varepsilon\sqrt{\pi}$ in order to satisfy the conditions (21) and (23). The final population transfer to the collective marked state is larger than 0.99. Top: Rabi frequencies. Bottom: populations of the collective marked (P_m), unmarked (P_u), and excited ($P_{e\perp}$) states as a function of dimensionless time.

there is a larger transient population in the upper state for the cases of Figs. 5 and 6; (ii) the population dynamics of the latter cases do not exhibit the oscillations noticed in Fig. 4. Both features can be interpreted using superadiabatic bases

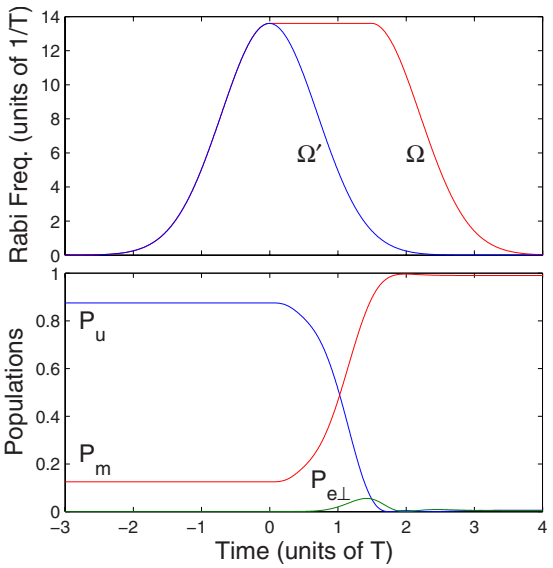

FIG. 5. (Color online) Numerical dynamics for the effective Hamiltonian (15) with $f=M/N=1/8$ and Rabi frequencies chosen as $\Omega'(t)=\Omega_0 e^{-(t/T)^2}$ and a Gaussian profile with a plateau for $\Omega(t)$ as in (34) in order to satisfy (21). Here $\Omega_0 T$ is such that the final population transfer to the marked state is 0.99. Top: Rabi frequencies. Bottom: populations of the collective marked (P_m), unmarked (P_u), and excited ($P_{e\perp}$) states as a function of dimensionless time.

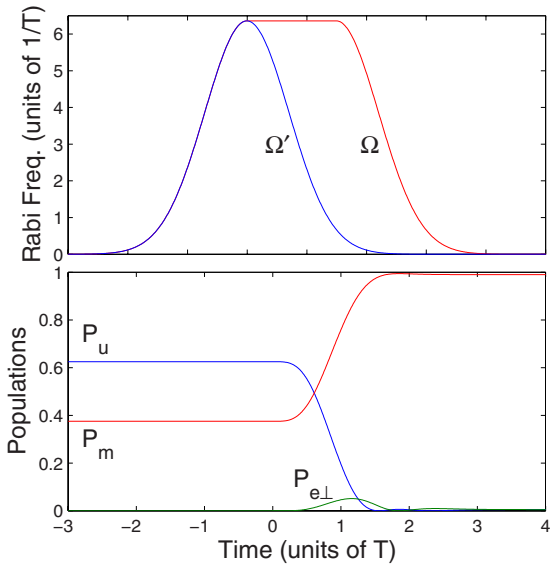

FIG. 6. (Color online) Same as Fig. 5, but with $f=M/N=3/8$.

that are better adapted to describe the dynamics [19,20]. This superadiabatic transport allows one to explain the final revival of the transient "lost" population in the upper state shown in Figs. 5 and 6 [21,22]. Furthermore, the use of analytic pulses in the cases of Figs. 5 and 6 explain the nonoscillatory transfer. For the preceding case, the local adiabatic control (23) induces the condition (26) which prevents in general the analyticity of one of the pulses (here Ω' if Ω is chosen analytic). In this nonanalytic case, through nonadiabatic transitions in a superadiabatic basis (of order related to the order of the discontinuous derivative), population transfer occurs in an oscillatory manner as shown in Fig. 4.

Figure 7 displays the scaling of the search duration T for the scheme which uses the pulses of the the form (34) as shown in the upper panel of Fig. 5. The duration of the plateau has been kept to $1.5T$ ($\alpha=1.5$), and the quantity $\Omega_0 T$ has been determined numerically from the requirement that the population transfer to the collective marked state reaches 0.99. We obtain a duration search scaling essentially as $f^{-0.53}$, which demonstrates the approximate quadratic speedup of the search.

Finally, we investigate the role of the plateau in the efficiency of the search. The scaling exponent β of the search duration for various plateau durations αT is analyzed in Fig. 8. For each value of α, the power β is determined numerically by a linear fit of the log-log representation of $\Omega_0 T$ as a function of $1/f$ (obtained in the same conditions as for Fig. 7). Figure 8 shows that the power β decreases to 0.53 as the dynamics becomes more adiabatic until $\alpha\approx 1.5$ before increasing slightly and saturating to 0.6 for $\alpha>2.5$.

Before concluding, let us make some remarks concerning the experimental implementation of this adiabatic Grover search. First, the scheme described here requires one to trap atoms in a cavity, a task which can be achieved, for instance, using a standing-wave dipole-force trap [23]. As a realistic Λ atomic scheme, we can consider the typical 2^3S_1-2^3P_0 tran-

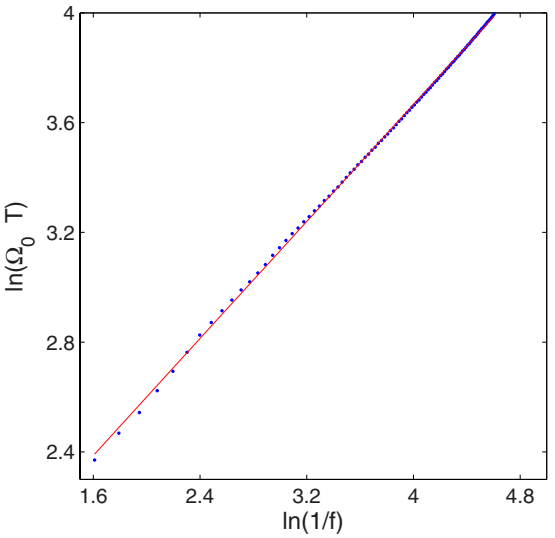

FIG. 7. (Color online) Scaling of $\Omega_0 T$, with T the process duration, as a function of the fraction f of solution for the search with tailored Gaussian pulses as in Fig. 5. The plateau duration is fixed to $1.5T$, and the final population of the collective marked state is 0.99. The natural logarithm of $\Omega_0 T$ as a function of the natural logarithm of $1/f$ obtained numerically (dotted line) is well fitted by the straight line of slope 0.53.

sition in metastable helium, which is of linewidth $\Gamma \sim 10^7$ s^{-1} and Rabi frequency $\Omega \sim 10^8 \sqrt{I}$ s^{-1} (with the intensity I in W/cm^2). In order to neglect spontaneous emission, as assumed in (2), we require the condition $(\Omega_0 T)^2 \gg \Gamma T$. It is fulfilled when $\Omega_0 T \gg 1$ and $\Omega_0 \gg \Gamma$, which are well satisfied in practice—e.g., for $I_0 \sim 10^4$ W/cm^2 and $T \sim 10$ ns. Finally, the feasibility of fixing the ratio of two pulses (here essentially required at early times in the local adiabatic conditions approach) has been shown in [24] using acousto-optical modulation of a cw laser in such a nanosecond regime. This step is not required in the other approach using Gaussian pulses with plateaus. One can mark the atoms by an ac Stark shift using a magnetic field—for instance, from a focused laser beam for spatial resolution.

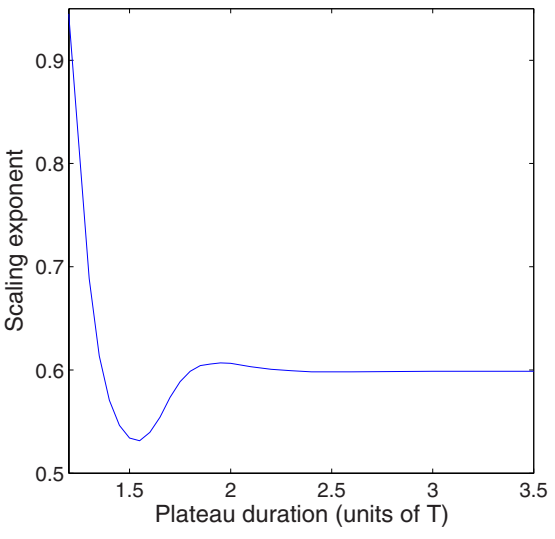

FIG. 8. (Color online) Power β of the scaling $f^{-\beta}$ of $\Omega_0 T$ as a function of the plateau durations αT for tailored Gaussian pulses. The scaling exponent β is obtained as in Fig. 7 (see text for details).

V. CONCLUSIONS

We have investigated theoretically a physical implementation of the adiabatic Grover search using a cavity-laser-atom system and robust processes related to STIRAP. The calculation has been conducted with pulses based on the constraint (23), which has allowed us to prove the scaling analytically. We have checked the robustness of the $f^{-1/2}$ scaling by numerical simulations using other less restrictive adiabatic pulse shapes satisfying (21). The case of Gaussian pulses with plateaus, which are routinely used in laboratories, has been studied. In particular, a scaling close to optimal is obtained when, after a Gaussian switching on, one of the two pulses is kept constant for a time equal to (or larger than) $3/2$ of its characteristic time. Finally, the experimental implementation of the presented scheme has been briefly discussed.

ACKNOWLEDGMENTS

The authors are grateful to N. J. Cerf and H.-R. Jauslin for useful discussions and acknowledge support from EU projects COVAQIAL and QAP, from the Belgian government program IUAP under Grant No. V-18, and from the Conseil Régional de Bourgogne. S.G. acknowledges support from the French Agence Nationale de la Recherche (ANR CoMoC).

APPENDIX: PARTITIONING

Let us consider a system whose Hilbert space is partitioned into two orthogonal Hilbert spaces by means of the projection operators $\mathcal{P}_A$ and $\mathcal{P}_B = 1 - \mathcal{P}_A$. The pertaining Hamiltonian can be written as

$$H = H_A + H_B + H_{AB} + H_{BA} \equiv H_A + H_B + \epsilon V, \qquad \text{(A1)}$$

where ϵ is a formal small (or more precisely ordering) parameter. The purpose is to achieve a perturbative block diagonalization of H. The leading contribution from the off-diagonal blocks to the diagonal ones can be extracted by the partitioning technique [25]. There is a unitary transformation $\exp(\epsilon W)$ such that

$$e^{-\epsilon W} H e^{\epsilon W} = H_A + H_B + \frac{1}{2}[\epsilon V, \epsilon W] + \epsilon^3 V', \qquad \text{(A2)}$$

with the property that $[\epsilon V, \epsilon W] = \mathcal{P}_A[\epsilon V, \epsilon W]\mathcal{P}_A + \mathcal{P}_B[\epsilon V, \epsilon W]\mathcal{P}_B$. The leading correction to the diagonal blocks is thus of order 2, while the remainder $(\epsilon^3 V')$ is of order 3. It has been shown that $\epsilon W = \epsilon W_{BA} - \epsilon W_{BA}^\dagger$, with ϵW_{BA} given by

$$\epsilon W_{BA} = -\sum_{j,k} \frac{|\lambda_j^B\rangle\langle\lambda_j^B| H_{BA} |\lambda_k^A\rangle\langle\lambda_k^A|}{\lambda_j^B - \lambda_k^A}, \qquad \text{(A3)}$$

where $|\lambda_k^A\rangle$ denotes the eigenvector of H_A corresponding to the eigenvalue λ_k^A (and similarly for H_B). Recall that ϵ is only

formally a small parameter (it can be set to 1). However, note from (A3) that ϵW_{BA} and the high-order terms in (A2) are smaller, the larger the differences in the eigenvalues of H_A and H_B.

We now apply these results to the Hamiltonian (12), taking H_1 for H, $\mathcal{P}_{e_\perp}$ for $\mathcal{P}_A$, and $\mathcal{P}_e$ for $\mathcal{P}_B$. The dominant contribution from the off-diagonal blocks $H_{e_\perp e}$ and $H_{ee_\perp}$ to $H_{e_\perp}$ is obtained from (A2),

$$H^{(2)}_{e_\perp} = H_{e_\perp} + \frac{1}{2}\mathcal{P}_{e_\perp}[\epsilon V, \epsilon W]\mathcal{P}_{e_\perp}$$

$$= H_{e_\perp} + \frac{1}{2}(H_{e_\perp e}\epsilon W_{ee_\perp} + \text{H.c.}), \tag{A4}$$

where $\epsilon W_{ee_\perp}$ is given by (A3). The eigenvalues of H_e are $\pm\sqrt{N}G$, and the corresponding eigenvectors read

$$|\pm\sqrt{N}G\rangle \equiv \frac{1}{\sqrt{2}}(|e,0\rangle \pm |g,1\rangle). \tag{A5}$$

In the resonant approximation ($\Sigma \equiv \Omega + e^{-i\delta t}\Omega' \approx \Omega$ and $\Sigma' \equiv \Omega' + e^{i\delta t}\Omega \approx \Omega'$), the eigenvectors of $H_{e_\perp}$ are

$$|0\rangle = \cos\theta|g'_{\text{m}},0\rangle - \sin\theta|g'_{\text{u}},0\rangle,$$

$$|\pm\Lambda\rangle = \frac{1}{\sqrt{2}}(\sin\theta|g'_{\text{m}},0\rangle + \cos\theta|g'_{\text{u}},0\rangle \pm |e_\perp,0\rangle), \tag{A6}$$

with the instantaneous angle θ defined through $\tan\theta \equiv -\sqrt{(1-f)/f}\Omega'/\Omega$ and

$$\Lambda \equiv \sqrt{(1-f)\Omega'^2 + f\Omega^2}. \tag{A7}$$

To determine the leading correction to $H_{e_\perp}$ given in (A4), we note that $H_{e_\perp e} = H_{e_\perp e}\mathcal{P}_e = H_{e_\perp e}|e,0\rangle\langle e,0|$. Hence, we simply have to compute $\langle e,0|\epsilon W_{ee_\perp}$, which after some algebra, reads

$$\langle e,0|\epsilon W_{ee_\perp} = \frac{\Lambda(\sqrt{f}\Omega'\sin\theta + \sqrt{1-f}\Omega\cos\theta)}{NG^2 - \Lambda^2}\langle e_\perp,0|$$

$$= \frac{\Lambda\sqrt{1-f}(\Omega^2 - \Omega'^2)\cos\theta}{(NG^2 - \Lambda^2)\Omega}\langle e_\perp,0|.$$

The correction featured in (A4) is then

$$H_{e_\perp e}\epsilon W_{ee_\perp} = \frac{\Lambda\sqrt{1-f}(\Omega^2 - \Omega'^2)\cos\theta}{(NG^2 - \Lambda^2)\Omega}$$

$$\times(\sqrt{f}\Omega'|g'_{\text{m}},0\rangle + \sqrt{1-f}\Omega|g'_{\text{u}},0\rangle)\langle e_\perp,0|. \tag{A8}$$

Recall that, by definition of the problem, the constraint imposed in this Grover search is that the pulse envelopes Ω and Ω' do not increase with N—i.e., are at most of order N^0. It then follows from (A7) that Λ is at most of order N^0. Note that the additional dependency on N introduced through f may only decrease Λ. As a consequence, the correction (A8) to $H_{e_\perp}$ decreases at least as $1/NG^2$ and may be discarded, giving rise to the effective Hamiltonian $H_{\text{eff}} = H_{e_\perp}$ defined in (15).

[1] L. K. Grover, Phys. Rev. Lett. **79**, 325 (1997).
[2] I. L. Chuang, N. Gershenfeld, and M. Kubinec, Phys. Rev. Lett. **80**, 3408 (1998).
[3] J. A. Jones, M. Mosca, and R. H. Hansen, Nature (London) **393**, 344 (1998).
[4] M. S. Anwar, D. Blazina, H. A. Carteret, S. B. Duckett, and J. A. Jones, Chem. Phys. Lett. **400**, 94 (2004).
[5] P. G. Kwiat, J. R. Mitchell, P. D. D. Schwindt, and A. G. White, J. Mod. Opt. **47**, 257 (2000).
[6] P. Walther, K. J. Resch, T. Rudolph, E. Schenck, H. Weinfurter, V. Vedral, M. Aspelmeyer, and A. Zeilinger, Nature (London) **434**, 169 (2005).
[7] K.-A. Brickman, P. C. Haljan, P. J. Lee, M. Acton, L. Deslauriers, and C. Monroe, Phys. Rev. A **72**, 050306(R) (2005).
[8] F. Yamaguchi, P. Milman, M. Brune, J. M. Raimond, and S. Haroche, Phys. Rev. A **66**, 010302(R) (2002).
[9] Z. J. Deng, M. Feng, and K. L. Gao, Phys. Rev. A **72**, 034306 (2005).
[10] E. Farhi and S. Gutmann, Phys. Rev. A **57**, 2403 (1998).
[11] V. L. Ermakov and B. M. Fung, Phys. Rev. A **66**, 042310 (2002).
[12] E. Farhi, J. Goldstone, S. Gutmann, and M. Sipser, e-print arXiv:quant-ph/0001106.
[13] A. M. Childs, E. Farhi, and J. Preskill, Phys. Rev. A **65**, 012322 (2001).
[14] J. Roland and N. J. Cerf, Phys. Rev. A **65**, 042308 (2002).
[15] D. Daems and S. Guérin, Phys. Rev. Lett. **99**, 170503 (2007).
[16] N. V. Vitanov, T. Halfmann, B. W. Shore, and K. Bergmann, Annu. Rev. Phys. Chem. **52**, 763 (2001).
[17] M. Fleischhauer and M. D. Lukin, Phys. Rev. A **65**, 022314 (2002).
[18] N. V. Vitanov, K.-A. Suominen, and B. W. Shore, J. Phys. B **32**, 4535 (1999).
[19] M. V. Berry, Proc. R. Soc. London, Ser. A **429**, 61 (1990).
[20] A. Joye and C.-E. Pfister, J. Math. Phys. **34**, 454 (1993).
[21] M. Elk, Phys. Rev. A **52**, 4017 (1995).
[22] K. Drese and M. Holthaus, Eur. Phys. J. D **3**, 73 (1998).
[23] S. Nussmann, M. Hijlkema, B. Weber, F. Rohde, G. Rempe, and A. Kuhn, Phys. Rev. Lett. **95**, 173602 (2005).
[24] V. A. Sautenkov, C. Y. Ye, Y. V. Rostovtsev, G. R. Welch, and M. O. Scully, Phys. Rev. A **70**, 033406 (2004).
[25] S. Guérin and H. R. Jauslin, Adv. Chem. Phys. **125**, 147 (2003).